00-101

Submitted to the *Proceedings of the Material Research Society 1999 Fall Meeting,* Boston, MA, November 29–December 3. 1999

Relationship Between Structure and Luminiscent Properties of Epitaxial Grown Y_2O_3:Eu Thin Films on $LaA1O_3$ Substrates

H-J. Gao, G. Duscher, X. Fan, and S. J. Pennycook
Solid State Division, Oak Ridge National Laboratory, Oak Ridge, TN

D. Kumar, K. G. Cho, P. H. Holloway, and R. K. Singh
Department of Materials Science and Engineering, University of Florida, Gainesville, FL 32611-6400

prepared by
SOLID STATE DIVISION
OAK RIDGE NATIONAL LABORATORY
Managed by
LOCKHEED MARTIN ENERGY RESEARCH CORP.
under
Contract No. DE-AC05-96OR22464
with the
U.S. DEPARTMENT OF ENERGY
Oak Ridge, Tennessee

RELATIONSHIP BETWEEN STRUCTURE AND LUMINISCENT PROPERTIES OF EPITAXIAL GROWN Y_2O_3:Eu THIN FILMS ON $LaAlO_3$ SUBSTRATES

H-J. GAO, G. DUSCHER, X.D. FAN, and S.J. PENNYCOOK, D. KUMAR*, K.G. CHO*, P.H. HOLLOWAY*, R.K. SINGH*
Solid State Division, Oak Ridge National Laboratory, Oak Ridge, TN 37831-6030
*Department of Materials Science and Engineering, University of Florida, Gainesville, FL32611-6400

ABSTRACT

Cathodoluminescence images of individual pores have been obtained at nanometer resolution in europium-activated yttrium oxide (Y_2O_3:Eu) (001) thin films, epitaxially grown on $LaAlO_3$ (001) substrates. Comparison with Z-contrast images, obtained simultaneously, directly show the "dead layer" to be about 5 nm thick. This "dead layer" is the origin of the reduced emission efficiency with increasing pore size. Pore sizes were varied by using different substrate temperatures and laser pulse repetition rates during film growth. These films are epitaxially aligned with the substrate, which is always Al terminated.

INTRODUCTION

Doped Y_2O_3 (YO) thin films are of major interest for electroluminescence device applications.[1-12] A detailed microscopic understanding of the effect of specific defects on luminescence and their correlation with growth conditions is highly desirable for maximizing luminescent efficiency. Two major sources of defects can be identified; first, threading dislocations nucleated at the film/substrate interface, and second, voids distributed throughout the active film thickness. In this paper, we therefore first review a recent atomic-resolution study of the YO/$LaAlO_3$ interface structure,[13] then demonstrate the relationship between pore structure and the luminescent properties. Using Z-contrast scanning transmission electron microscopy (STEM)[14], we directly observe the nanometer-scale cathodoluminescence (CL) of the film, and show that the reduction in luminescent efficiency is due to a "dead layer" around each pore caused by strong recombination of electron-hole pairs at the internal pore surfaces.

Eu-activated YO thin films were deposited by laser ablation[15-17] on (001) $LaAlO_3$ (LAO) substrates. For details see ref.18. Rocking curve measurements indicate a full width half maximum (FWHM) of 0.1°. Cross-sectional slices were obtained by cutting the LAO along the [100] or [010] directions (using pseudocubic indexing) and then gluing face to face in the usual way. Both plan-view and cross-section specimens were prepared for transmission electron microscopy (TEM) and/or STEM observations by mechanical grinding, polishing, and dimpling, followed by Ar-ion milling.

TEM bright field images and electron diffraction patterns were recorded in a Philips EM-400 electron microscope operated at 100kV. High-resolution Z-contrast imaging was conducted in a VG HB603U STEM at 300kV,[14,19] while the cathodoluminescent (CL) imaging was carried out in a VG HB501 STEM at 100 kV. The CL emission was collected by a lens system and detected by a photomultiplier, as shown in the schematic of Fig. 1.

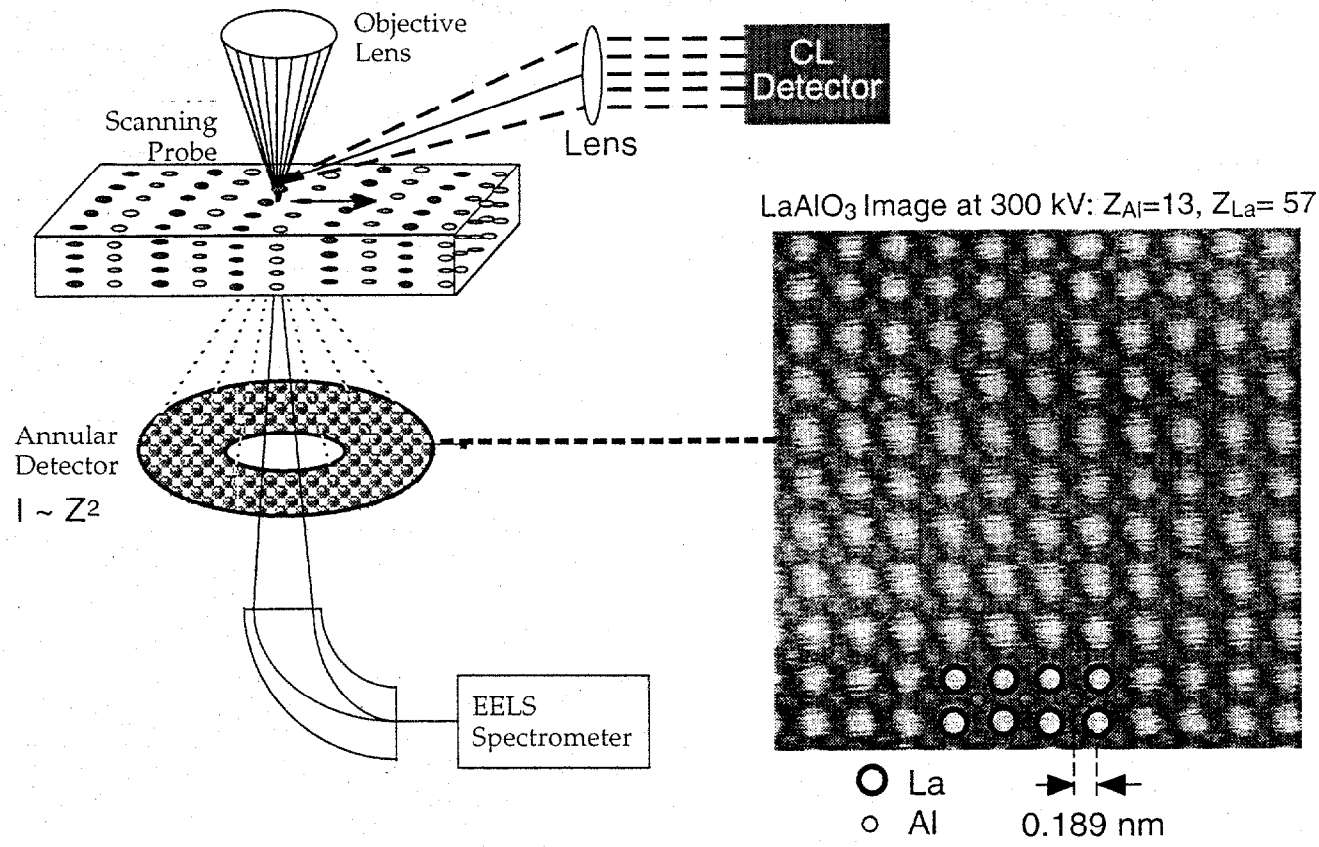

Fig. 1 Schematic of the Z-contrast scanning transmission electron microscope (STEM) imaging together with the cathodoluminescent imaging system

FILM/SUBSTRATE INTERFACE STRUCTURE

It is well known that Y_2O_3 has a C-type rare-earth sesquioxide structure, closely related to the fluorite structure with a cell parameter a=1.060 nm and space group T_h^7(Ia3).[20-23] In the fluorite lattice, each cation is surrounded by eight anions located at the corner of a cube. The C-type structure is derived by removing one-quarter of oxygen atoms and slightly rearranging the remaining ones.[24] For 75% of the cations the vacancies lie at the ends of a face diagonal, while for the other 25% they lie at the ends of a body diagonal. Therefore, each yttrium atom is surrounded by only six oxygen neighbors forming two different types of distorted octahedral structure in the unit cell, called S_6 and C_2.[25] Eight yttrium atoms have the S_6 symmetry and the other 24 atoms have the C_2 symmetry. From the crystallographic structure one can deduce that the distance of two neighboring Y atoms along the <100> direction of YO is 0.5302 nm, and along the <110> direction is 0.375 nm. LAO is a rhombohedral structure with lattice parameters **a** = 0.378 nm, $\theta \approx 90.5^{\circ}$, very close to a cubic structure. The lattice mismatch with the <110> direction of the YO is therefore less than 0.8%, and so we would anticipate epitaxial growth of single crystalline YO thin films on the LAO (001) substrate to be feasible.

Figure 2 is a low magnification TEM micrograph and corresponding selected area diffraction (SAD) pattern of a plan view sample of the YO:Eu thin film. The diffraction pattern indicates an almost perfect single crystal film, but the image shows numerous small voids, suggesting an island growth mechanism with incomplete coalescence of the islands. An image of the cross section sample is presented in Figure 3 (a), showing the smooth surface, sharp interface and a uniform thickness of 300 nm maintained over the entire region. Figure 3 also

shows SAD patterns of the film (b) and the LAO substrate (c), showing the orientation relationship to be [110]YO//[100]LAO and [-110]YO//[010]LAO. The columnar structure of the film is also apparent from the cross section image, with small rotations between neighboring grains giving the strong diffraction contrast. Each individual column however appears to be a good single crystal, which implies that the presence of the voids may avoid the need for a high density of dislocations between the grains to accommodate the rotations, and/or a high level of stress within the grains. The dominant direction of the voids is not crystallographic, suggesting that it is related to the deposition direction not being normal to the substrate.[26] The sample was not rotated during film deposition.

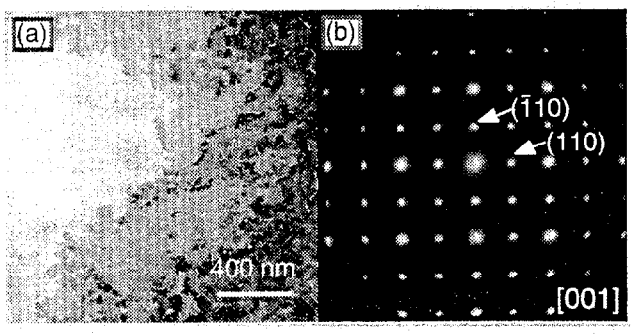

Fig. 2 Plan view TEM image (a) and corresponding electron diffraction pattern (b) of a laser-ablation-deposited YO:Eu thin film, showing the formation of a good single crystalline film containing numerous voids. The electron projection is along the [001] zone axis of the YO.

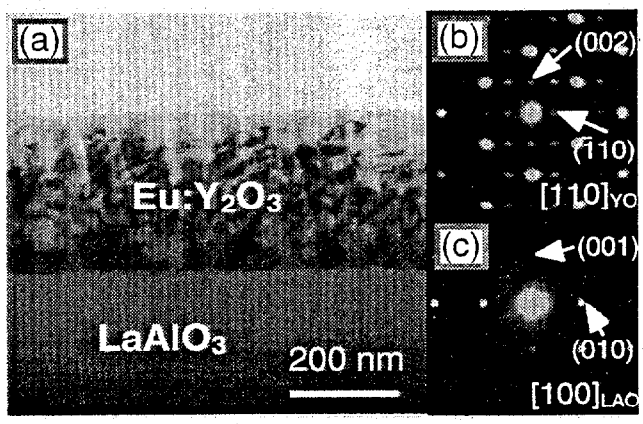

Fig. 3 Cross section TEM image (a) and corresponding SAD patterns of the as-grown YO:Eu film (b) and the LAO substrate (c) showing the orientation relationship to be [110]YO//[100]LAO and [-110]YO//[010]LAO.

In order to determine the detailed interfacial atomic structure, high-resolution Z-contrast STEM imaging of the samples was carried out. The Z-contrast image is a direct image with intensity highly localized about the atomic column positions and approximately proportional to the mean square atomic number (Z). Thus the La and Al columns in LAO, and the Y columns in YO, are directly distinguishable in a Z-contrast image taken along the [010] zone axis of the LAO substrate. Figure 4(a) is an atomic resolution Z-contrast STEM image of the film/substrate interface. The bright spots in the film are Y columns; in the substrate the brightest spots La columns, and the less-bright spots are Al columns. The O columns are not visible. Also shown in Fig. 4(b) is a higher magnification Z-contrast image that shows clearly the atomic structure of the interface. The substrate is seen to terminate with the Al plane, which matches directly onto the Y layer of the film as shown in the schematic.

Figure 5 is a schematic of two possible interface structures corresponding to the two possible terminations of the (001) substrate, either the $(AlO_2)^-$ or $(LaO)^+$ planes. Figures 5 (c) and (d) show these two planes, while (e) and (f) show the two (001) planes of YO, comprising pure Y and O. The full unit cell of the YO structure is four times the dimensions shown due to ordering of the O vacancies. For $(AlO_2)^-$ termination of the substrate, the four oxygen positions match almost exactly the oxygen positions in the YO. The Y atoms can sit over the center of the four O positions in Fig. 5(d), directly over the La site in the plane below, as seen in the image of Fig. 4(b). The interfacial Y is then coordinated by seven oxygen atoms instead of six, which may be compensated by some additional oxygen vacancies. In contrast, if the substrate is

terminated by LaO, each Y sitting directly over one oxygen in the LaO plane, then each Y is substantially undercoordinated. This explains the observed termination and the fact that no single layer height steps were observed.

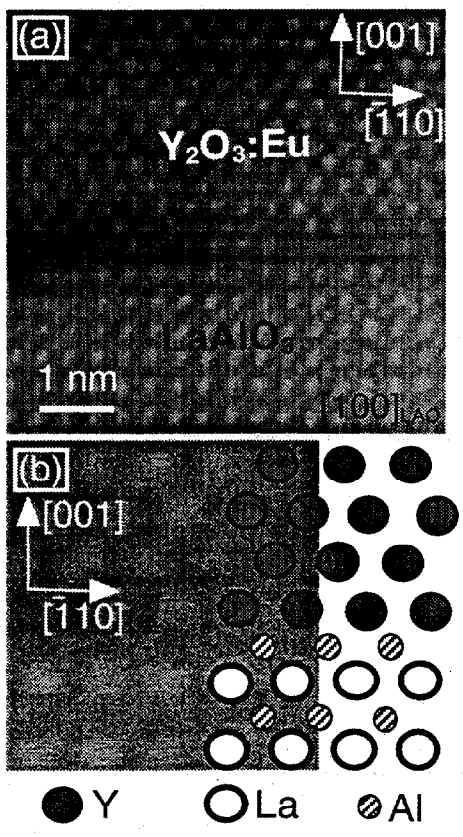

Fig. 4 (a) Z-contrast STEM dark field image showing the atomically abrupt interface, (b) higher magnification image showing clearly the Al terminated substrate, as shown in the schematic.

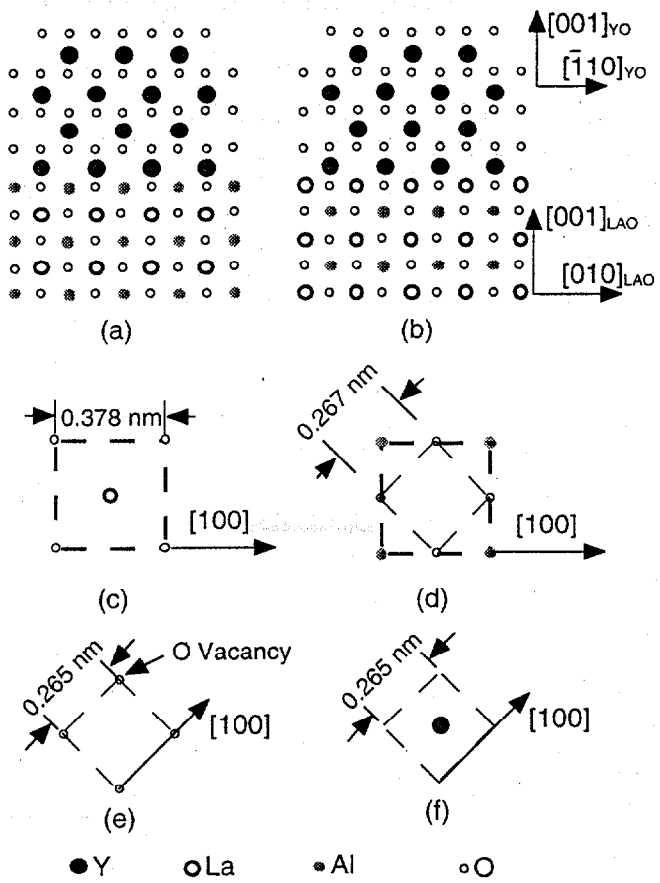

Fig. 5 Schematic interface structures for YO on the Al terminated surface (a), and on the La terminated surface of LAO (b). Atomic arrangements on the substrate (001) surface are shown for La termination (c), and Al termination (d). The atomic arrangements on the alternating oxygen and Y {004} planes in YO are shown in (e) and (f).

CORRELATION OF MICROSTRUCTURE TO LUMINESCENCE PROPERTIES

The variation of film microstructure with growth conditions is shown in Fig. 6. The size of the pores increases with lower substrate temperatures and higher pulse rates. The photoluminescent efficiency correlates directly with average pore size, as shown in Fig. 7, and we would expect the CL efficiency to be similar. The reason for this correlation is expected to be the existence of a "dead layer" near the specimen surface, resulting from non-radiative recombination of electron-hole pairs via surface states. Increasing pore size would create more internal surfaces per unit volume, resulting in lower overall efficiency.

Direct measurement of the "dead layer" at the surface of a pore has been achieved by comparing the Z-contrast image with the CL image obtained simultaneously. Fig. 8 (a) shows a Z-contrast image of a region of film containing some relatively widely spaced pores. The corresponding CL image (b) shows the variation in CL intensity. It is immediately clear that the edges of the holes in the CL image are much less sharp. Intensity profiles across the hole marked are shown in Fig. 8(c) and (d). The width of the pore in the Z-contrast image is 10 nm, whereas in the CL image it is more than doubled to 20 nm. Clearly if the grain size of a film is comparable to the extent of the dead layer, then the efficiency will be substantially reduced. This explains the order of magnitude reduction in efficiency for the sample shown in Fig. 6(a), in which the grain size is ~30 nm. It is clear that because of this "dead layer," porous structures can lead to greatly reduced emission efficiencies.

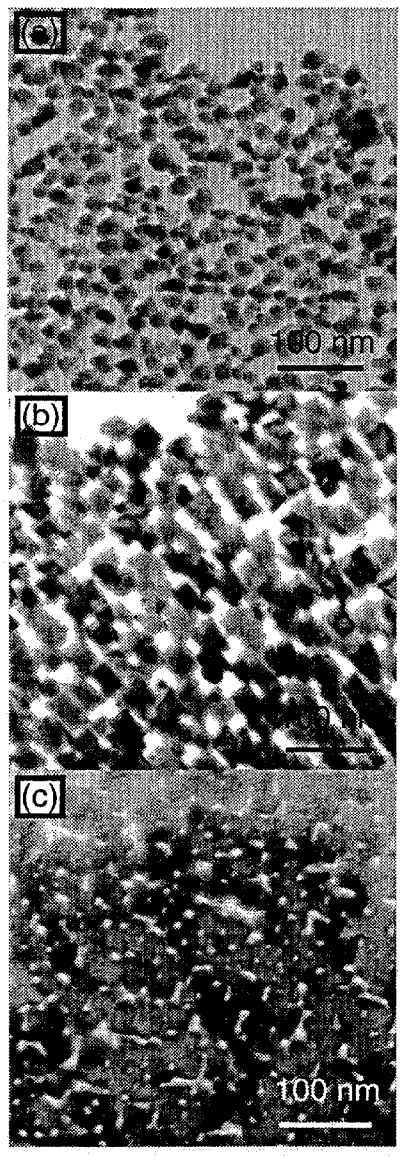

Fig. 6. Plan view TEM micro-graphs of Y_2O_3:Eu thin films grown at 735 °C (a, b) or 775 °C (c), with laser pulse frequency 10 Hz, (a,c) or 5 Hz (b).

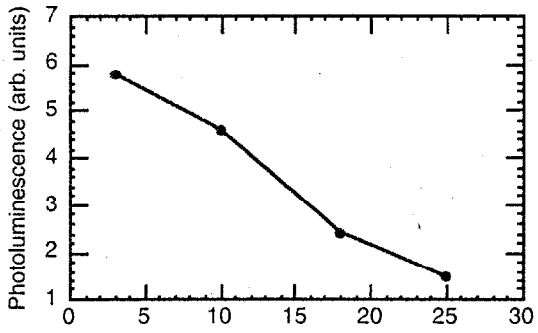

Fig. 7. Relationship between the average pore size and the photoluminescent efficiency.

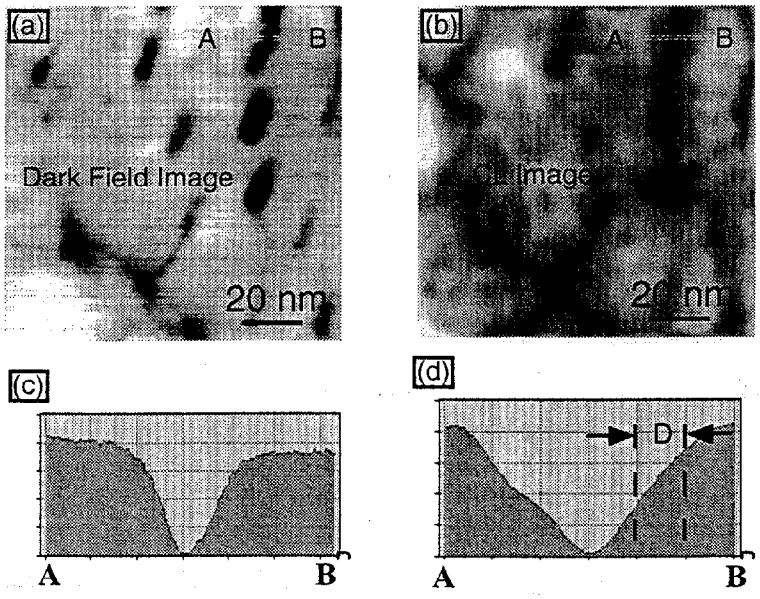

Fig. 8. Z-contrast image (a) and corresponding CL image (b) of the specimen shown in Fig. 6(c). Intensity profiles across the single pore from A to B are shown in (c) and (d) revealing the CL dead layer (D) to extend for about 5 nm.

ACKNOWLEDGEMENTS

The authors are grateful to A. Kadavanich for assistance with the CL detection system. The work at ORNL was sponsored by the Division of Materials Sciences, U.S. Department of Energy, under Contract No. DE-AC05-96OR22464 with Lockheed Martin Energy Research Corporation, and by appointment to the ORNL Postdoctoral Research Program administrated jointly by ORISE and ORNL. The work at University of Florida was supported by the Phosphor Technology Center of Excellence by DARPA Grant No. MDA972-93-1-0030.

REFERENCES

1. L. Manchanda and M. Gurvitch, IEEE Electronic Devices Lett. **9**, 180(1988).
2. T.S. Kalkur, Y.R. Kwor, and C.A. Paz de Araujo, Thin Solid Films **170**, 185(1989).
3. S.J. Duclos, C.D. Greskovich, and C.R. O'Clair, MRS Symp. Proc. **348**, 503(1994).
4. G.Blasse and B.C. Grabmaier, *Lum. Mater.* Springer, Berlin(1994).
5. S.C. Choi, M.H. Cho, S.W. Whangbo, C.N. Whang, S.B. Kang, S.I. Lee, and M.Y. Lee, Appl. Phys. Lett. **71,** 903(1997).
6. R.P. Rao, Solid State Communications **99,** 439(1996).
7. K.-I. Onisawa, M. Fuyama, K. Tamura, K. Taguchi, T. Nakayama, and Y.A. Ono, J. Appl. Phys. **68**, 719(1990).
8. A.F. Jankowski, L.R. Schrawyer, and J.P. Hayes, J. Vac. Sci. Technol. **A11**, 1548(1993).
9. W.M. Cranton, D.M. Spink, R. Stevens, and C.B. Thomas, Thin Solid Films **226**, 156(1993).
10. S.L. Jones, D. Kumar, R.K. Singh, and P.H. Holloway, Appl. Phys. Lett. **71**, 404(1997).
11. K.G. Cho, D. Kumar, D.J. Lee, S.L. Jones, P.H. Holloway, and R.K. Singh, Appl. Phys. Lett. **71**, 3335(1997).
12. K.G. Cho, D. Kumar, S.L. Jones, D.J. Lee, P.H. Holloway, and R.K. Singh, J. Electrochem. Soc. **145**, 3456(1998).
13. H-J. Gao, D. Kumar, K.G. Cho, P.H. Holloway, R.K. Singh, X.D. Fan, Y. Yan, and S.J. Pennycook, Appl. Phys. Lett. **75**, 2223(1999).
14. S. J. Pennycook, "STEM: Z-contrast", in *Handbook of Microscopy*, ed. By S. *Amelinckx, D. van Dyck, J. van Landuyt, and G. van Tendeloo*, VCH Publishers, Weinheim, Germany, pp. 595 (1997).
15. J. Fitz-Gerald, S.J. Pennycook, H. Gao, V. Krishnamoorthy, J. Marcinka, W. Glenn, R. Singh, Mat. Res. Soc. Proc. Spring 1998, **502**, (1998).
16. J. Fitz-Gerald, T. Trottier, R.K. Singh, P.H. Holloway, Appl. Phys. Lett. **72**, 1838(1998).
17. D. Kumar, J. Fitz-Gerald, R.K. Singh, Appl. Phys. Lett. **72**, 1451(1998).
18. H-J. Gao, et al., Appl Phys. Lett. (to be published).
19. N.D. Browning, M. F. Chisholm, S.J. Pennycook, Nature **366**, 143(1993).
20. J.L. Daams, P. Villars, and J.H.N. Vanvucht, *Atlas of Crystal Structure types for Intermetallic Phases*, P.6706. ASM International, Materials Park. OH(1994).
21. M.G. Paten and E.N. Maslen, Acta. Crystallogr. **19**, 307(1965).
22. B.H. O'Conner, T.M. Valentine, Acta Crystallogr. **B25**, 2140(1969).
23. M. Faucher, J. Pannetier, Acta Crystallogr. **B36**, 3209(1980).
24. W.v. Schaik and G. Blasse, Chem. Mater. **4**, 410(1992).
25. F. Jollet, C. Noguera, N. Thromat, M. Gautier, and J.P. Duraud, Phys. Rev. B **42**, 7587(1990).
26. E.S. Machlin, *Materials Science in Microelectronics*, Giro Press, Croton-on-Hudson (1995).